The Investigation of Gas Ejector Performance using CFD Modelling

Kemal Aldas [1], Faruk Şen [2], Iskender Ozkul [1]

[1]*Aksaray University Faculty of Engineering, 68100, Aksaray, Turkey*
[2]*Muğla Sıtkı Koçman University Department of Energy Systems Engineering 48000, Muğla, Turkey.*

Abstract **– Computational fluid Dynamics (CFD) has been widely used to simulate the experimental studies, which cost a lot of time and need to be repeated many times, in different fields of the industry with sufficient accuracy results. Therewithal, the energy conservation and controlled use of energy is very important for the more clean and habitable world. Therefore, refrigerant gases used in cooling systems should not affect global warming and damage to the ozone layer. Regarding that, in this study the ejector performance was mapped in Computational Fluid Dynamics (CFD) software using R600a (isobutene) refrigerant gas that the hydrocarbon-based, non-ODP (Ozone Depletion Potential) and has less effect of GWP (Global Warming Potential).**

Keywords- **Ejector, CFD, R600a, Cooling, Modelling**

1. Introduction

In recent years, the Computational Fluid Dynamics (CFD) simulation technique is considerably developed and extended its scope of application and began to provide more accurate results. In the modern applications with CFD gives sufficiently accurate results even in the strong shocks and the optimization of the gas ejectors [1],[2],[3].

The ejector is a device that transfers momentum from a high velocity primary jet flow to a secondary flow. It is geometrically simple since it consists of four main components namely, nozzle, suction chamber, mixing throat and diffuser as schematically shown in Figure 1. Ejectors has pivotal advantages such as easy to install, being economic usage, lack of moving parts, bearing components, lubrication sealing problems, etc.. Therefore, the ejectors are used in a reliable way to transports for gases, liquids and solid components in many engineering and industrial applications.

Ejectors can be used in the heating and cooling systems using the solar energy. Regarding that, there are a lot of numerical and experimental studies in the literature [4-10]. Additionally, many studies are available on the modelling of constant field and constant-pressure suction chambers on the ejectors [11], [12]. Keenan et. al [13] expressed to obtained better performances where the mixing takes place in constant pressure suction chamber. The various refrigerants were used in studies on the ejectors [14-17]. Presently, refrigerant gases that have less GWP effect and non-ODP have been studied [18],[19]. In this study, R600a refrigerant gas which has less GWP effect and non-ODP was selected.

2. CFD modelling

The turbulence flow model in the simulations which R600a is selected as primary and secondary (entrained) fluid was used the realizable k-ε turbulence model. Because, the model has been validated extensively for a wide range of flows, including free flows, jets, mixing layer, channel, boundary layer flows and separated flows. Especially, it predicts more accurately the spreading rate for axisymmetric (round) jets, [20]. Flow within a gas is a combination of such flows in which the underlying physics is very complex. In analyzing the gas ejector by CFD the following assumptions are done:(i) flow within ejector is steady and compressible, (ii) heat transfer between gas and surroundings doesn't exist, (iii) surface roughness is taken as zero, (iv) effect of buoyancy is neglected. Based on these assumptions, continuity, momentum and energy equations can be written as:

$$\frac{\partial}{\partial x_i}\left(\rho u_i\right) = 0 \tag{1}$$

$$\frac{\partial}{\partial x_i}\left(\rho u_i u_j\right) = \frac{\partial P}{\partial x_i} + \frac{\partial \tau_{ij}}{\partial x_j} \tag{2}$$

$$\frac{\partial}{\partial x_i}\left(u_i\left(\rho E + P\right)\right) = \vec{\nabla}.\left(\alpha_{eff}\frac{\partial T}{\partial x_i}\right) + \vec{\nabla}.\left(u_j\left(\tau_{ij}\right)\right) \tag{3}$$

Where

$$\tau_{ij} = \mu_{eff}\left(\frac{\partial u_i}{\partial x_j} + \frac{\partial u_j}{\partial x_i}\right) - \frac{2}{3}\mu_{eff}\frac{\partial u_k}{\partial x_k}\delta_{ij} \tag{4}$$

The transport equations for the realizable k-ε Turbulence model become as follows:

$$\frac{\partial}{\partial x_j}\left(\rho k u_j\right)=\frac{\partial}{\partial x_j}\left[\left(\mu+\frac{\mu_t}{\sigma_k}\right)\frac{\partial k}{\partial x_j}\right]+G_k-\rho\varepsilon \quad (5)$$

$$\frac{\partial}{\partial x_j}\left(\rho\varepsilon u_j\right)=\frac{\partial}{\partial x_j}\left[\left(\mu+\frac{\mu_t}{\sigma_\varepsilon}\right)\frac{\partial \varepsilon}{\partial x_j}\right]+\rho C_1 S\varepsilon-\rho C_2\frac{\varepsilon^2}{k+\sqrt{\nu\varepsilon}} \quad (6)$$

Where the production of turbulence kinetic energy G_k is modelled as:

$$G_k=\mu_t S^2 \quad (7)$$

Other terms: $C_1=\max\left[0.43,\frac{\eta}{\eta+5}\right]$, $\eta=S\frac{k}{\varepsilon}$,

$$S=\sqrt{2S_{ij}S_{ij}} \text{ and } S_{ij}=\frac{1}{2}\left(\frac{\partial u_j}{\partial x_i}+\frac{\partial u_i}{\partial x_j}\right) \quad (8)$$

The model constants for this case;

$$C_2=1.9,\quad \sigma_k=1.0,\quad \sigma_\varepsilon=1.2$$

These default values were used in the present simulations.

In the realizable k-ε turbulence model suited to compute flows within gas ejector, turbulent or eddy viscosity, μ_t, is not constant and it is calculated from

$$\mu_t=\rho C_\mu\frac{k^2}{\varepsilon} \quad (9)$$

Where C_μ varies depending on turbulence fields, the mean strain and rotation rates and the angular velocity of the system.

In order to achieve a more accurate definition of the turbulent flow the three-dimensional geometry model was used in this study. The computational domain was reduced by half using a symmetry plane to decrease the calculation time and the mesh number. To obtain the mesh-independent solution the adaptive meshing method was applied and maximum number of cells for a half volume of ejector within jet pump was around 125045. Results of the grid sensitivity analysis for optimum operating conditions are given in Table 2. P_g generator pressure, T_g generator temperature inlet boundary conditions were used for the motive and P_e evaporator pressure and T_e evaporator temperature entrained flows and P_c condenser pressure, T_c condenser temperatures outlet boundary conditions for the mixed (exit) flow were implemented to define the flow domain and then the mass flow rates of primary, secondary and mixed flows were computed using the coupled solution algorithm for pressure-velocity coupling, the quick scheme for spatial discretisation and the pressure-based solver. The convergence criteria for continuity, momentum and transport (model) equations were always less than 10^{-4} and iterations were continued until the convergence criteria were satisfied. Results of sensitivity analysis of the iterative convergence criteria for optimum operating conditions are given in Table 2. (4) (5)

3. Results and discussion

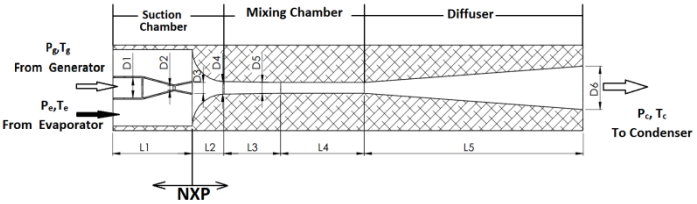

Figure 1. Schematic diagram of the ejector

D1	*D2*	*D3*	*D4*	*D5*	*D6*	*L1*	*L2*	*L3*	*L4*	*L5*
8	3.12	4.8	11	9.5	19	30	14	25	36.8	96.5

Table 1. Ejector dimensions (mm)

Mesh number	M_r	*Convergence Criteria*	M_r
40526	0.824	0.001	0.823
125045	0.821	0.0001	0.839
226309	0.821	0.00001	0.831

Table 2. Sensitivity analysis based on the mass flow ratio (6)

An additional parameter, affecting the performance of the ejector is jet distance that NXP. The mass flow rates were plotted by the different jet distance according to T_g=100°C, T_c=26°C and Te=12°C in Figure 2. As seen in the Figure 2, the best performance results between NXP -5mm and 25 mm is 15 mm.

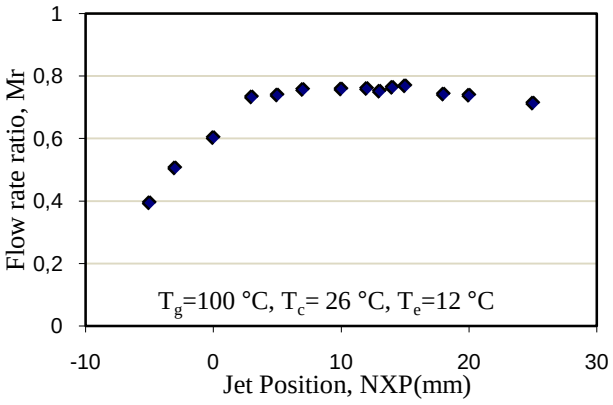

Figure 2. Flow rate ratio of depending on NXP

At 90°C generator temperature, evaporator temperature at 12°C and three different condenser temperatures of turbulence intensity are plotted in Figure 3. As shown in figure intensity of turbulence rises suddenly in the evaporator temperature at 28°C in constant pressure region and abruptly decreases at the end of this area. Because of these conditions, the fluid exchange of energy is not observed between the primary flow and secondary flow. The reduction intensity of turbulence in the mixing chamber is derived the absence of secondary fluid. The condenser temperatures at 26°C, the turbulence intensity rises towards the end of mixing section so exchange of energy is kept between the motive fluid and suction fluid. When the temperature of condenser is 22°C, the mixture of energy exchange continues till the first part of the diffuser. This also proves us that the suction process is carried out exactly.

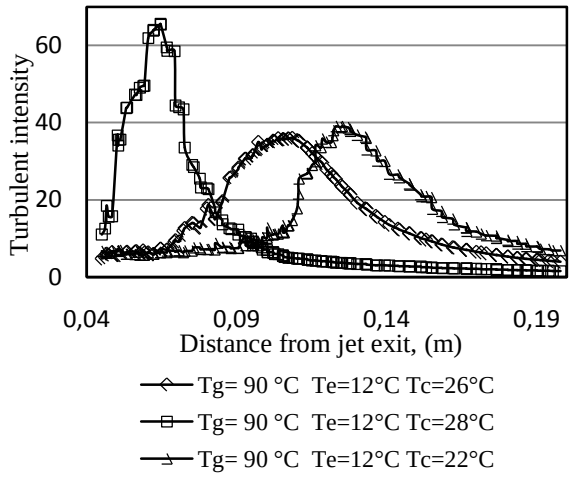

Figure 3. Turbulence intensity values of different T_c

In Figure 4, the static pressure distribution was plotted along the axis from the jet exit. The fluctuation was observed in the ejector mixing section at NXP distance in different values of static pressure. The static pressure fluctuations do not appear inside the mixing section at optimum NXP=15 mm value. At NXP=15 mm, the amount of secondary fluid rises in the mixing section and two-fluid enters the diffuser in equilibrium case by exchanging energy. The early fluctuation of static pressure at other nozzle positions shows the non-equilibrium between primary and secondary flow.

In this case, the ejector performance is affected. The turbulence in the mixing section shows that the shock was occurred at the inlet of the mixing section. The energy exchanges of these shocks were not completed exactly. As a result of that, the ejector performance reduced.

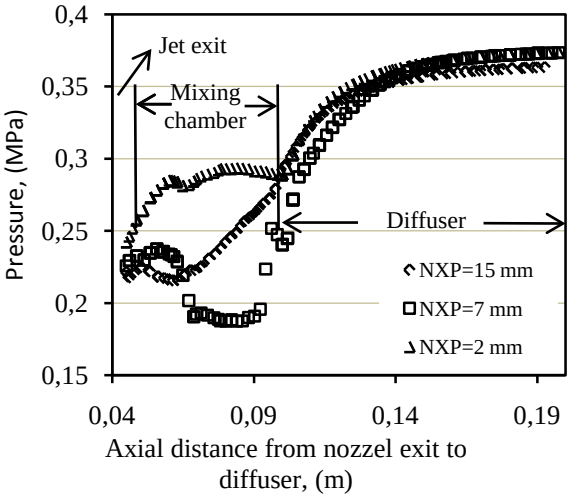

Figure 4. Pressure distribution from nozzle exit to diffuser

In Figure 5 a, b and c, the mass flow rates were plotted according to different generator temperatures. As can be seen in the figure, flow rate remains constant until condenser temperature reaches a critical T_{cr} temperature in a constant fixed primary flow. When the temperature exceeds T_{cr} temperature, the mass flow rate suddenly decreases. The reason of remain constant flow rate at low T_c temperatures is choking of the primary, secondary flow. The first choking occurs in the primary nozzle. The second choking, at the entrance of mixing section, the primary flow brings the secondary flow velocity to speed of sound in this region. Therefore, the mass flow rate does not change. Ejector mass flow rate is inversely proportional to condenser pressure. If the condenser pressure is lower than critical pressure, two choking occurs in the system and the mass flow rate doesn't change. Also as shown in figure 5, the mass flow rate decreases with increasing generator temperature at constant temperature of secondary flow. Thus, the primary flow temperature and pressure should be selected according to the condenser temperature for best performance of the ejector.

Otherwise a part of the energy will be wasted.

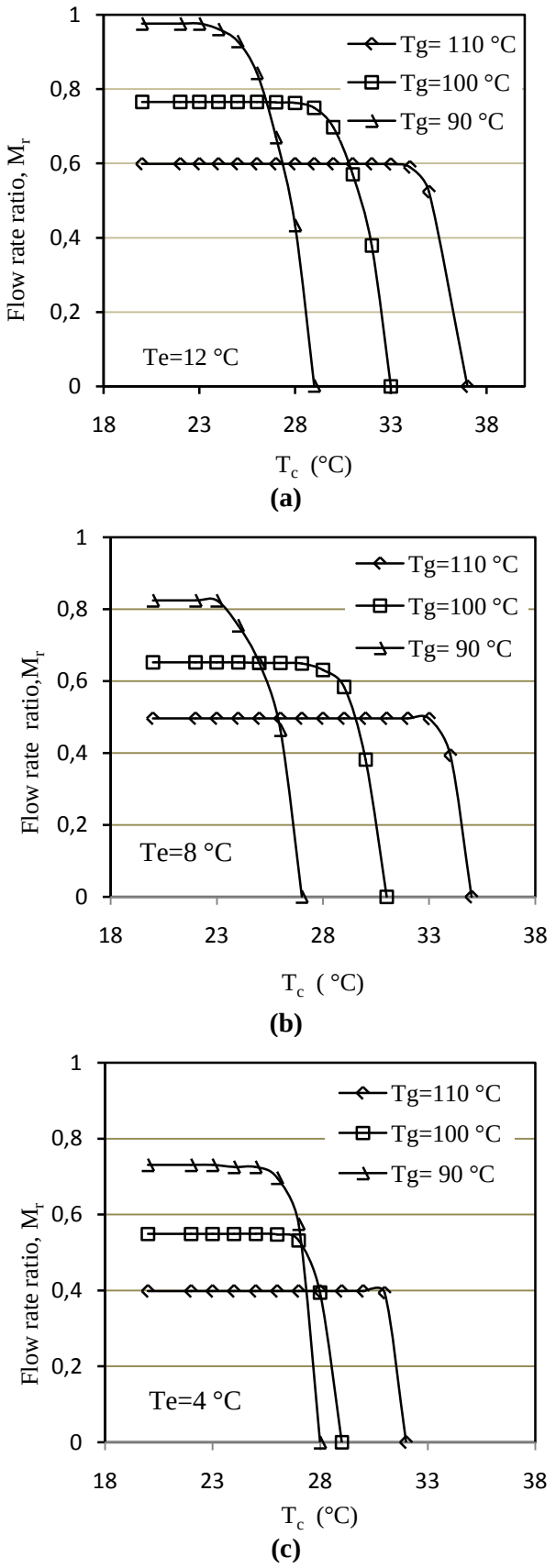

Figure 5. Flow rate ratio change at the different evaporator temperatures

In figure 6, according to different condenser temperatures at 22°C, 26°C, 28°C and 30°C, contours velocity were plotted. As can be seen in the figure the flow over sound speed, contour length shortens with the condenser temperature and pressure rises. In Figure 6 a, the formation of shock along to end of the mixing section does not prevent the exchange of energy between two fluids because of lower condenser temperature T_c than the critical T_{cr} temperature. In addition, as shown in figure choking of secondary flow was observed at first part of mixing section due to unchanged the mass flow profiles. During condenser temperature approaches the critical temperature, the shock wave moves forward in mixing section and it prevents to choke of secondary flow and then mass flow rate begins to decrease. If the condenser pressure is increased furthermore, the reverse flow consists on system as shown in Figure 6-d.

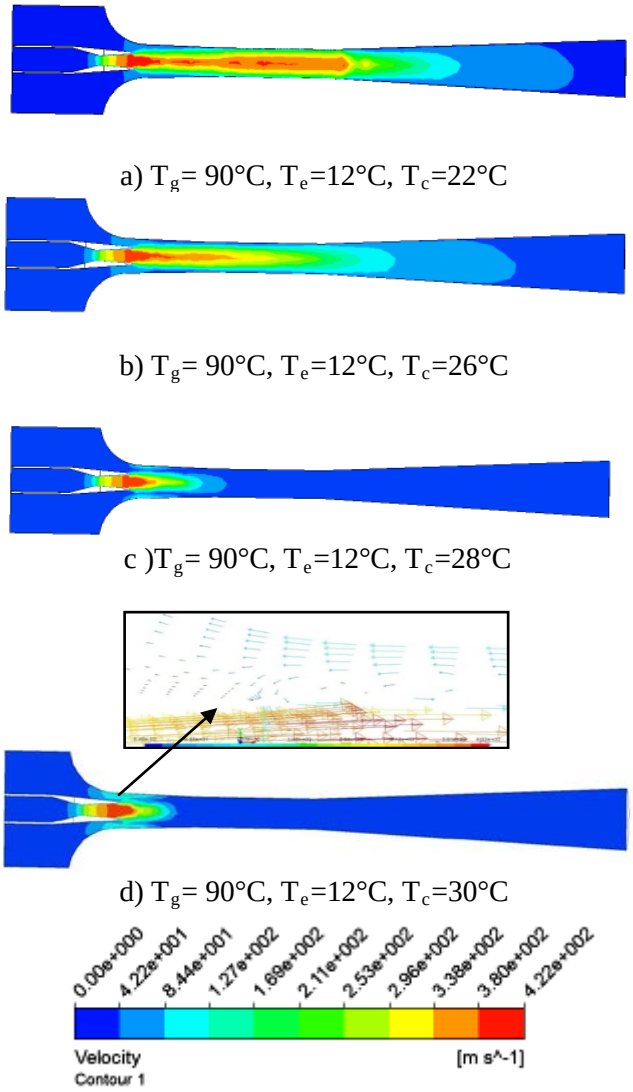

Figure 6. Velocity contours at various T_c condenser temperatures with constant T_g and T_e

In figure 7, according to different condenser temperatures at 22°C, 26°C 28°C and 30°C, Mach number were plotted. As the figure shows during condenser temperature raises, the Mach number decreases at other condenser temperatures except for 22°C after exit of the jet. The mach number remains approximately horizontal as shown in the figure beginning from the jet exit to end of the mixing section at T_c = 22°C. The shock develops at the end of mixing section due to the condenser pressure is lower than the critical pressure so it doesn't affected the mixture fluid. At the same time this explains us choking the suction fluid. Due to the condenser temperature, the Mach number begins to decrease if condenser pressure is increased in the mixing section, so shock occurs towards the entrance of mixing section. This shows us that is not a good mixture in this region. If the condenser temperature continues to increase, reverse flow occurs. This is indicated by the values of T_c =30°C. Mach number reduced sharply at the entrance of mixing chamber.

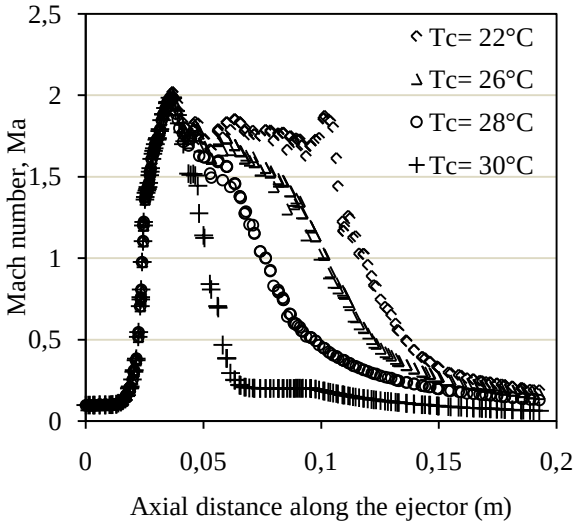

Figure 7. Mach number changes along the ejector

In the figure 8, the ejector operation mapped for R600a at distance of NXP 15 mm. In this section, at the generator temperature (T_g) from 90°C to 110°C, at evaporator temperature (T_e) between 4°C and 12°C and at condenser temperature (T_c) between 20°C and 35°C temperatures show varies. As shown in the figure with increasing T_g temperature, the critical condenser temperature increases at the same T_e temperature but the mass flow rate decrease. Also as increasing T_e temperature at fixed temperature of T_g, the flow rate and critical temperature of the condenser increase.

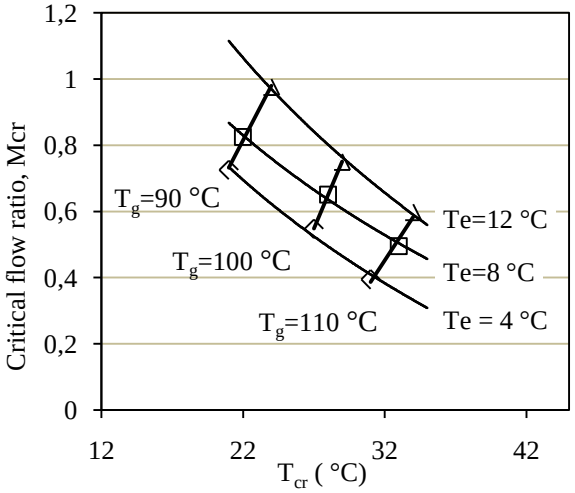

4. Conclusion

In this study, the ejector operating was investigated with Computational Fluid Dynamics (CFD) using various generator, evaporator and condenser temperatures, with R600a gas, throat diameter of 3.12 mm, suction chamber diameter of 9.5 mm. The results of the study following comments were presented;

- The Ejector performance is affected by NXP and the condenser temperature values. NXP value becomes smaller, the suction does not take place completely and the shock waves are composed in regions close to the entrance of mixing chamber. These conditions affect the performance of the ejector.

- At the same generator temperature and till critical condenser temperatures the amount of the mass flow rate (M_r) does not change. However, if temperature of the diffuser out port exceeds the critique of condenser temperature, mass flow rate (M_r) decreases.

- Up to the critical temperature, Mach number remains at about the same level in mixing chamber. If The critical temperature is continued to increase, it consists a sudden decrease in Mach number because of reverse flows.

- Increasing temperature of T_c at the fixed temperatures of T_g and T_e, turbulence intensity increases. In this case there are no sufficient energy exchange between the primary flow and secondary flow.

References

[1]. Li C, Li YZ, *Investigation of entrainment behavior and characteristics of gas–liquid ejectors based on CFD simulation*. Chemical Engineering Science 66(3):405-416. 2011.

[2]. Fan J, Eves J, Thompson HM, Toropov VV, Kapur N, Copley D, Mincher A, *Computational fluid dynamic analysis and design optimization of jet pumps*. Computers & Fluids 46: 212–217. 2011.

[3]. Hemidi A, Henry F, Leclaire S, Seynhaeve J M, Bartosiewicz Y, *CFD analysis of a supersonic air ejector. Part I: Experimental validation of single-phase and two-phase operation.* Applied Thermal Engineering 29: 1523–1531. 2009.

[4]. Bajmak S, Milenkovic D, *Experimental Analysis of Main Characteristics Ejectors, Comparative Analysis of Experimental Data Calculatedly characteristics*, TEM Journal- Volume 2 / Number 1/ 2013.

[5]. Utomo T, Jin Z, Rahman MS, Jeong H,Chung H, *Investigation on hydrodynamics and mass transfer characteristics of a gas-liquid ejector using three-dimensional CFD modeling*. Journal of Mechanical Science and Technology 22, 1821–182.2008.

[6]. Wang J, Dai Y, Gao L, Ma S,A *New combinedcooling,heating and power system driven by solar energy*, Renewable Energy 34, 2780-2788.2009.

[7]. Zhang XJ, and Wang RZ, *A new combined adsorption-ejector refrigeration and heating hybrid system powered by solar energy*, Appl Therm Eng.,22,1245-1258.2002.

[8]. Sun DW, *Variable geometry ejectors and their applications in ejector refrigeration systems*, Energy, 21,10; 919-929.1996.

[9]. Vidal H, Colle S,and Perira SG, *Modelling an hourly simulation of solar ejector cooling system*, Applied Thermal Engineering 26,663-672. 2006.

[10]. Varga S, Oliveira AC, Diaconu B, Numerical *assessment of steam ejector efficiencies using CFD.* International Journal of Refrigeration 32, 1203–1211. 2009.

[11]. Riffat SB, Holt A, *A noval heat pipe/ejector cooler*, Appl. Therm. Eng. 18(3-4) 93-101.1998.

[12]. Huang BJ, Chang JM, Wang CP, Petreko VA, *A 1-D analysis of ejector performance*, Ing.J. Refrigerat 22,354-364.1999.

[13]. Keenan JH, Neumann EP,Lusstwerk F, *An investigation of ejector design by analysis and experiment*, ASME J. Appl. Mech. Trans. 299-309.1950.

[14]. Boumnaraf L, Lallemand A, *Modeling of an ejector refrigerating system operating in dimensioning and off-dimensioning conditions with the working fluids R142b and R600a*, Appiled Thermal Engineering 29,265-274.2009.

[15]. Selvaraju A, Mani A, *Analysis of an ejector with environment friendly refrigerants,*Appl. Therm. Eng. 24,827-838.2004.

[16]. Cizingu K, Mani A, Groll M, *Performance comparison of vapour jetrefrigeration system with environmentally friendly working fluids*, Appl.Therm. Eng. 21,585–595. 2001.

[17]. Dorantes R, Lallemand A, *Prediction of performance of a jet cooling system operating with pure refrigerants or non-azeotropic mixtures,* Int. J. Refrigerat. 18,vol:1, 21–30.1995.

[18]. Pridasawas W, Lundqvist P, *A year-round dynamicsimulation of solar-driven ejector refrigeration system withiso-butane as a refrigerant* Int. J. Refrigeration 30,840-850.2007.

[19]. Nehdi E, Kairouani L, Elakhdar M, *A solar ejector airconditioning system using environment-friendly working fluids*. Int. J. Energ. Res. 32, vol:13,1194-1201.2008.

[20]. ANSYS, Inc. Theory Guide .ANSYS FLUENT 14.0, 2009.

Corresponding author*: Iskender ÖZKUL*
Institution: *Aksaray University Faculty of Engineering, 68100, Aksaray, Turkey*
E-mail: *iskender@aksaray.edu.tr*